

## **A Solar Wind Model with Current Sheets**

G. Li<sup>1,2</sup> and G. Qin<sup>3</sup>

<sup>1</sup> *Department of Physics, University of Alabama Huntsville, AL 35899*

<sup>2</sup> *CSPAR, University of Alabama Huntsville, AL 35899*

<sup>3</sup> *State Key Laboratory of Space Weather, Center for Space Science and Applied Research, Chinese Academy of Sciences, Beijing 100190, China*

**Abstract.** Current sheets are common structures in the solar wind and are a significant source of solar wind MHD turbulence intermittency. They can arise from non-linear interactions of MHD turbulence or be relic structures in the solar wind that having a solar origin. Observations show that magnetic field directions often change abruptly upon crossing these structures. The presence of these structures can affect the transport of solar energetic particles. To understand the effects of these current sheet a realistic solar wind model that includes them is necessary. In this work, we construct a realistic solar wind model that explicitly includes current sheets. In our model, the solar wind is composed of individual cells with varying local uniform mean magnetic fields. The size of the individual cells are adjusted to agree with in-situ observations at 1 AU. The turbulence in each cell is modeled by either a slab and/or 2D turbulence.

### **1. Introduction**

A central topic of the solar wind MHD turbulence is intermittency. In a collisionless plasma such as the solar wind, intermittency arises because the fluctuations of magnetic field or fluid velocity are not scale invariant as conjectured in the first hydrodynamic turbulence theory (Kolmogorov 1941) (hereafter K41 theory). Observationally, a very important intermittent structure in the solar wind is current sheet. A current sheet is a 2D structure where the magnetic field direction changes significantly from one side to the other. Bruno et al. (2001) studied current sheets using Helios 2 data at 0.9 AU. They performed a minimum variance analysis to study how the solar wind magnetic field vector evolves for several selected time periods. By plotting the trajectory of the tip of the magnetic field vector in the minimum variance reference system, Bruno et al. (2001) showed that the magnetic field direction at times undergo abrupt changes, implying the presence of current sheet. Furthermore, Bruno et al. (2001) have also proposed the possibility that most of these flux tubes might be of solar origin and, as such, advected by the wind. The analysis of Bruno et al. (2001) showed that current sheets are common in the solar wind and they may be the boundaries of flux tubes. However, there are alternative views about the origin of current sheets. Numerical MHD simulations by Zhou et al. (2004) showed that current sheets emerge as the dynamical evolution of the nonlinear interactions of the solar wind MHD turbulence, i.e. the generation of current sheet can be spontaneous. Similarly study by Chang et al. (2004) also showed that starting from an isotropic initial MHD turbulence state, non-linear interactions in

the solar wind can lead to the emergence of various coherent structures, including current sheet. These studies (Zhou et al. 2004; Chang et al. 2004) suggested that current sheet is an *intrinsic* property of the solar wind MHD turbulence. In contrast, advocating Bruno et al. (2001)'s idea, Borovsky (2008), on examining one-year worth magnetic field data from the ACE spacecraft, has found a clear signature of two population of current sheets with one extending to large angle separations. Borovsky (2008) suggested that these current sheets are the “magnetic walls” of flux tubes in the solar wind and they are *relic* structures which can be traced back to the surface of the Sun. In this picture, current sheets are carried out by the solar wind as passive structures. The plasma in the solar wind are bundled in “spaghetti-like” flux tubes. Indeed, solar wind consisting of “spaghetti-like” flux tubes has been suggested by Bartley et al. (1966) and McCracken and Ness (1966) as an attempt to explain the modulation of cosmic rays and later adopted by Mariani et al. (1973) to explain the observed variations in the occurrence rate of discontinuities in interplanetary magnetic field.

Extending the work of Borovsky (2008), Li (2007, 2008) developed a systematic method to identify current sheets in the solar wind. The essence of the method is to study the  $\zeta$ -scaling properties of the angle  $\theta = \cos^{-1}(\hat{B}(t) \cdot \hat{B}(t + \zeta))$ . This method allows one to show statistically the existence of current sheets. Li (2008) further presented a method to obtain the exact location of individual current sheets. Following Li (2007, 2008), Miao et al. (2011) developed an automatic data analysis procedure to identify current sheets in the solar wind. The procedure can obtain the location and the width (thickness) of individual current sheets and the deflection angle of the magnetic field across the current sheet. By studying the waiting time analysis on these current sheets, it also gives a proxy of the flux tube size.

The effects on these current sheets on the transport of solar energetic particles were first investigated by Qin and Li (2008). In (Qin and Li 2008), we developed a toy model of the solar wind which is consist of individual cells and studied the effects of boundaries of these cells on the transport of solar energetic particles. We found that flux tubes in the solar wind can lead to stronger scatterings of particles in both directions parallel and perpendicular to the large scale background magnetic field. In particular a true diffusion in the large scale perpendicular direction (with respect to  $B_0$ ) can be obtained even when the local *intrinsic* turbulence in individual cells are of pure slab geometry.

In this paper, We improve our toy “cell model” developed in (Qin and Li 2008). We consider explicitly how the local magnetic field directions differ from the large scale background magnetic field. A procedure for obtaining the local magnetic field directions is given through the model parameters  $\theta$  and  $\phi$  (see below). By adjusting  $\theta$  and  $\phi$ , we fit our model results with that obtained from realistic solar wind observations at 1 AU.

## 2. Model description

As in (Qin and Li 2008), we assume the solar wind is composed of small cells with random size. Adjacent cells are separated by magnetic walls. We ignore the thickness of magnetic walls, therefore the change of magnetic field direction is modeled as sharp kinks (Qin and Li 2008). In every individual cell, the magnetic field is consist of a uniform mean magnetic field  $B_0^{local}$  and a turbulent magnetic field  $\delta B$ . The direction of  $B_0^{local}$  is assumed to be different from the direction of the underlying large scale

background field  $\mathbf{B}_0$ . For simplicity we assume the magnitude of  $B_0^{local}$  is the same magnitude as  $\mathbf{B}_0$ . To obtain the individual cells, we assume the size of the solar wind to be modeled occupies a space  $M_0$ . We next divide  $M_0$  into two smaller pieces by cutting  $M_0$  through an inner point  $P$  inside  $M_0$ . We recursively apply the cutting procedure  $N_p$  times and obtain  $p = 2^{N_p}$  smaller convex polyhedron cells. Denote these as  $M_1^i$  where the subscript 1 denotes the level and the superscript  $i$  denotes the cells at the corresponding level. For level 1,  $i$  is from 1 to  $p$ . Clearly, the sizes of different  $M_1^i$  are different and they are decided by how we identify  $P$ s.

Once we obtain all  $M_1^i$  (a total of  $p$  of them), we then select  $q$  ( $q < 8$ ) of them to perform the next level of cutting. Clearly, this step is of fractal in nature since the cutting is only done for  $\frac{q}{p}$  of  $M_1^i$ 's. Therefore  $\frac{q}{p}$  can be regarded as the space filling factor for the cutting process. In this work we choose  $N_p = 3$ , so  $p = 8$ . We also choose  $q = p$ , i.e. the cutting process is applied to *all* sub-polyhedrons from level  $i$  to  $i + 1$ . The final solar wind model is obtained when we recursively apply the above cutting procedure to a level of  $L$ , where a total number of  $N = p^L$  convex polyhedron cells are obtained. Clearly, how we choose the point  $P$  can affect the distribution of the size of the individual cells. In general for any given polyhedron  $M_l^i$  at level  $l$ , one can decide  $P$  through,

$$P_{x,y,z} = \frac{\sum_G w(G)G_{x,y,z}}{\sum_G w(G)} \quad (1)$$

where the summation is for all grid points  $G$  inside  $M_l^i$ ,  $w(G)$  is a number between 0 and 1 and represents the relative weights of point  $G$  in deciding  $P$ ;  $x$ ,  $y$  and  $z$  are the Cartesian coordinates. In (Qin and Li 2008),  $w(G) = 1$  is assumed. Such a choice corresponds to cutting the  $M_l^i$  through the center as close as possible. In this work, we choose  $w(G)$  such that the points close to the boundary of  $M_l^i$  have larger weights than points closer the center of  $M_l^i$ . This is to obtain the best comparison with observation.

Figure 1 is a 2D cartoon to illustrate our ‘‘cell model’’. The large scale background magnetic field is denoted by the arrow on the right. In individual cells, the local  $\mathbf{B}_0^{local}$ s are shown as the small arrows, whose directions differ from  $\mathbf{B}_0$ . Note all lengths are scaled to the local *intrinsic* turbulence correlation scale  $\lambda$ .

Once individual cells are obtained, we next decide the local background magnetic field  $\mathbf{B}_0^j$ . Let  $\mathbf{B}_0^j = B_0 \hat{z}'$  ( $j = 1$  to  $N$ ) then the direction  $\hat{z}'$  can be decided by two angles  $\theta = \cos^{-1}(\hat{z} \cdot \hat{z}')$  and  $\phi = \cos^{-1}(\hat{x} \cdot (\hat{z}' - \cos\theta \hat{z}))$  where the angle  $\theta$  and  $\phi$  represents the bending and the twisting of the local magnetic field  $\mathbf{B}_0^j$  from the large scale background magnetic field  $\mathbf{B}_0$ , respectively. We obtain  $\theta$  and  $\phi$  according to the following formulae:

$$p(\theta) = \frac{1 - \eta}{\sqrt{\pi}\alpha_1} \exp\left[-\left(\frac{\theta}{\alpha_1}\right)^2\right] + \frac{\eta}{\sqrt{\pi}\alpha_2} \exp\left[-\left(\frac{\theta}{\alpha_2}\right)^2\right], \quad (2)$$

$$p(\phi) = 1/360 \quad (3)$$

where,  $\eta = 0.036$ ,  $\alpha_1 = 16.9^\circ$ , and  $\alpha_2 = 45.5^\circ$ . Physically, equation (2) represents that the ‘‘bending’’ of the local magnetic field direction from the background magnetic field direction is given by two Gaussian distribution; and equation (3) represents that the ‘‘twisting’’ of the local magnetic field direction from the background magnetic field direction is given by a random distribution.

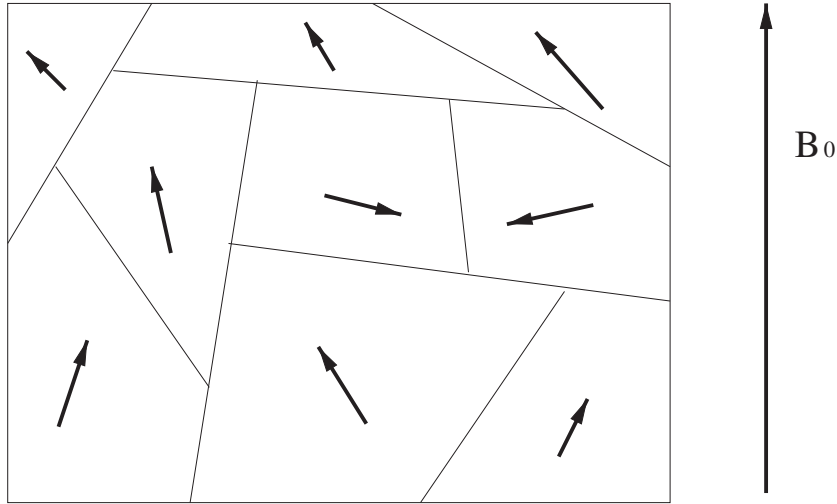


Figure 1. Cartoon showing our model of the solar wind. The background magnetic field is denoted by  $B_0$ . In each cell, a local background  $B_0^{local}$  is represented by the arrow, whose direction differs from  $B_0$ . For illustration purpose, this cartoon is in 2D. Adapted from (Qin and Li 2008).

## 2.1. Modeling a real solar wind

To describe the real solar wind, we first normalize our cell model to  $L \times L \times L$  where  $L = 0.06$  AU. This choice of  $L$  allows us to study the diffusion of energetic particles near 1 AU in the energy range of 0.1 MeV/nuc to 100 MeV/nuc (Qin and Li 2011). To model a real solar wind with current sheets, we focus on the following two properties of the current sheets from observation. The first is the distribution of the deflection angle of magnetic field direction between adjacent cells and the second is the distribution of cell size. Both of these are statistical quantities and have been studied by Miao et al. (2011) for Ulysses observations and Miao and Li (2010) for ACE observations. For the model to describe a realistic solar wind, it should yield similar distributions for both quantities.

To compare with observations at 1 AU, we have experimented different functional forms for  $\theta$  and  $\phi$ . The forms shown in formulae (2) and (3) yield reasonably good agreements with observations for the above two statistical quantities.

Consider first the deflection angle  $\Delta\theta$  distribution between adjacent flux tubes. At 1 AU, following the method presented in (Miao and Li 2010; Miao et al. 2011), the deflection angle  $\Delta\theta$  distribution for the year of 2005 and 2006 are obtained using ACE magnetic field data (Miao and Li 2011). For our model, we can obtain the same quantities by flying an imaginary spacecraft through our model solar wind and calculate the corresponding distributions. We consider multiple imaginary trajectories and obtain the distribution of the deflection angles for our model solar wind. Figure 2 plots the observed and modeled distribution of the deflection angle. The  $x$ -axis is the deflection angle in degree. The  $y$ -axis is the relative probability. It is normalized to the number of current sheets observed in year 2005 and 2006 by ACE. The diamonds are observation data points (Miao and Li 2011) and the solid line is our model. As discussed in (Miao et al. 2011), the deflection angle tends to have two population, both exponential decays,

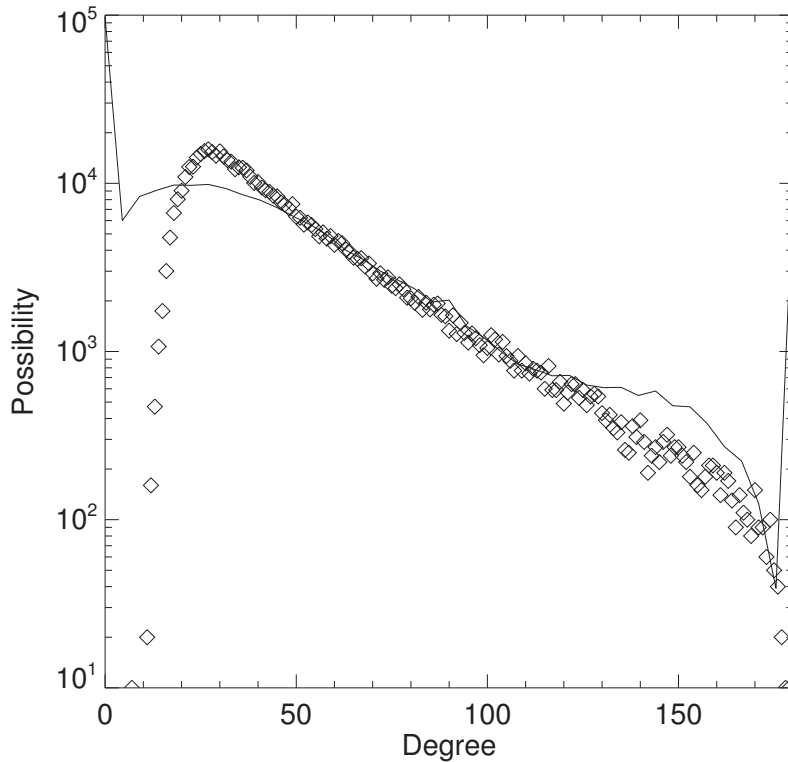


Figure 2. The distribution of the deflection angle of the magnetic field direction between adjacent cells. The diamonds are observation data points (Miao and Li 2011) and the solid line is our model.

with the first dominating at smaller angles ( $< 70^\circ$ ) and the second dominating at larger angles ( $> 70^\circ$ ). The one dominating at smaller angles decays faster and likely originates from local turbulence. The one dominating at larger angles decays slower and likely originates from flux tubes that are relic structures from the solar surface (Miao et al. 2011). Since we are interested in fluxtube boundaries, we therefore focus on modeling the second population of the observed deflection angle. From the figure we can see that our model agrees well with the observation at deflection angles ( $> \sim 70^\circ$ ). At smaller angles, as expected, our model yields a smaller probability. Next, we consider the waiting time analysis between the current sheets. If current sheets are the boundaries of flux tubes, then the waiting time between these current sheets can be used as a proxy of the size of the flux tubes. As shown in (Miao et al. 2011), the waiting time analysis of solar wind current sheets show a non-Poisson characteristics and therefore reveals the clustering tendency of the current sheets. By following the same imaginary trajectories as discussed above, we calculate the waiting time statistics from our model and compare it with observations. Figure 3 shows the waiting time analysis. The  $x$ -axis is in meter by assuming a solar wind speed of 400 km/s. The  $y$ -axis is the probably density. The dashed line is from observation and the solid line is from our model. What is remarkable

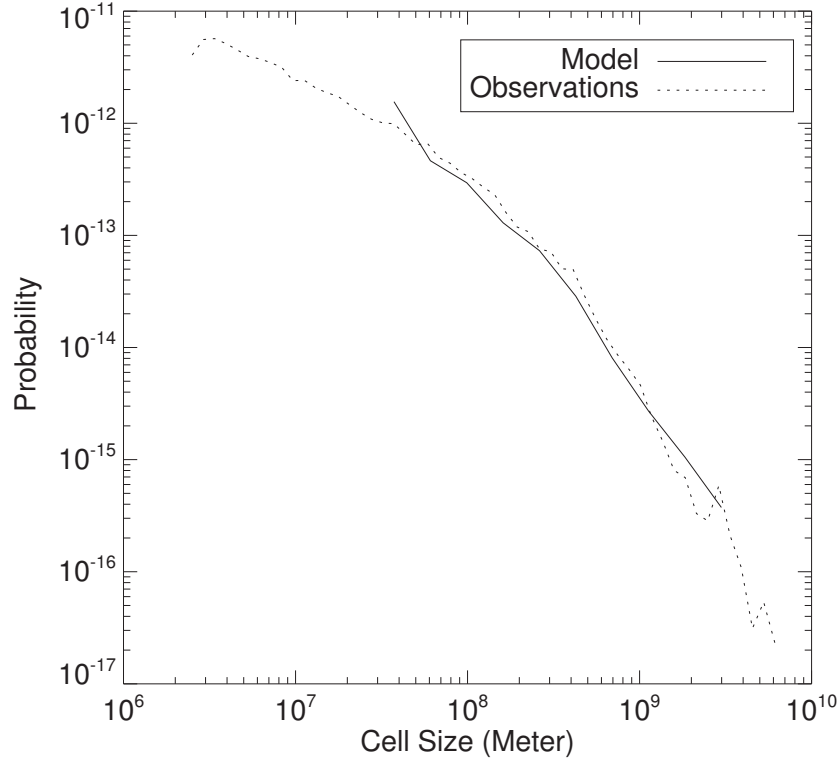


Figure 3. The waiting time distribution, which is also a proxy of the cell size distribution.

in figure 3 is that over two orders of magnitude, the waiting time distribution of our model agrees nicely with the observation.

### 3. Conclusion

We present in this paper a solar wind model which for the first time explicitly includes current sheets. We assume that the solar wind is consist of individual cells whose boundaries are the current sheets. The magnetic field directions in each cells are assumed to be different from the background large scale magnetic field but the magnitude to be the same. The direction deviation is described by two angles,  $\theta$  and  $\phi$ . By adjusting the sampling methods for  $\theta$  and  $\phi$ , we fit the modeled distribution of angle deflection across current sheets as well as the distribution of the cell size to the solar wind observation at 1 AU. As shown in figure 2 and figure 3, our model agrees well with observations, therefore provides a reasonably good approximation of solar wind. Our solar wind model presented here can be used as a basis for investigating transport of solar energetic particles Qin and Li (2011).

**Acknowledgments.** The authors acknowledge partial supports from NSF grant AGS-0962658 (SHINE) and NASA grant NNX07AL52A (EpSCoR). GL also likes

to acknowledge support from an ORAU Ralph E Power Junior Faculty Enhancement Award.

### References

- Bartley, W. C., Bukata, R. P., McCracken, K. G., and Rao, U. R. 1966, *J. Geophys. Res.*, 71, 3297
- Borovsky, J.E. 2008, *J. Geophys. Res-Space Phys.*, 113, 10.1029/2007JA012684.
- Bruno, R., Carbone, V., Veltri, P., Pietropaolo, E., & Bavassano, B. 2001, *Planet. Space Sci.*, 49, 1201
- Chang, T., Tam, S. W. Y., Wu, C-C 2004, *Phys. Plasmas*, 11,1287
- Kolmogorov, A. 1941, *C. R. Acad. Sci. URSS*, 30, 301
- Li, G. 2007, in AIP Conf. Proc. 932, *Turbulence and Nonlinear Processes in Astrophysical Plasmas*, ed. D. Shaikh & G. P. Zank (New York: AIP), 26
- Li, G. 2008, *ApJ*, 672, L65
- Mariani, F., Bavassano, B., Villante, U., and Ness, N. F. 1973, *J. Geophys. Res.*, 78, 8011
- McCracken, K. G., and Ness, N. F. 1966, *J. Geophys. Res.*, 71, 3315
- Miao, B., Peng, B., and Li, G., 2011, *Ann. Geophys.*, 29, 237-249.
- Miao, B. & Li, G. 2010, <http://www.srl.caltech.edu/ACE/ACENews/ACENews133.html>
- Miao, B. & Li, G., 2011, to be submitted.
- Qin, G. & Li, G., 2008, *ApJ*, 682: L129.
- Qin, G. & Li, G., 2011, *ApJ*, to be submitted.
- Zhou, Y., Matthaeus, W.H. and Dmitruk, P. 2004, *Rev. Mod. Phys.* 76, 1015